Neurobiology of Disease 183 (2023) 106157

Contents lists available at ScienceDirect

Neurobiology of Disease

journal homepage: www.elsevier.com/locate/ynbdi

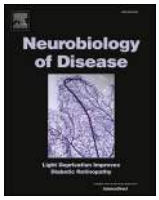

A mitochondrial-targeted antioxidant (MitoQ) improves motor coordination and reduces Purkinje cell death in a mouse model of ARSACS

Brenda Toscano Márquez [a], Tsz Chui Sophia Leung [a], Jeanette Hui [a], François Charron [b], R. Anne McKinney [b,*], Alanna J. Watt [a,*]

[a] Department of Biology, McGill University, Montreal, QC, Canada
[b] Department of Pharmacology and Therapeutics, McGill University, Montreal, QC, Canada

ARTICLE INFO

Keywords:
Ataxia
Autosomal-recessive spastic ataxia of the Charlevoix-Saguenay
ARSACS
MitoQ
Mitochondria
Purkinje cell
Cerebellum
Cerebellar nuclei
Mouse model of disease

ABSTRACT

Mitochondrial deficits have been observed in animal models of Autosomal-recessive spastic ataxia of Charlevoix-Saguenay (ARSACS) and in patient-derived fibroblasts. We investigated whether mitochondrial function could be restored in *Sacs*$^{-/-}$ mice, a mouse model of ARSACS, using the mitochondrial-targeted antioxidant ubiquinone MitoQ. After 10weeks of chronic MitoQ administration in drinking water, we partially reversed motor coordination deficits in *Sacs*$^{-/-}$ mice but did not affect litter-matched wild-type control mice. MitoQ administration led to a restoration of superoxide dismutase 2 (SOD2) in cerebellar Purkinje cell somata without altering Purkinje cell firing deficits. Purkinje cells in anterior vermis of *Sacs*$^{-/-}$ mice normally undergo cell death in ARSACS; however, Purkinje cells numbers were elevated after chronic MitoQ treatment. Furthermore, Purkinje cell innervation of target neurons in the cerebellar nuclei of *Sacs*$^{-/-}$ mice was also partially restored with MitoQ treatment. Our data suggest that MitoQ is a potential therapeutic treatment for ARSACS and that it improves motor coordination via increasing cerebellar Purkinje cell mitochondria function and reducing Purkinje cell death.

1. Introduction

Autosomal-recessive spastic ataxia of Charlevoix-Saguenay (ARSACS) is a neurodegenerative disorder caused by mutations in the gene *SACS* (Bouchard et al., 1978; Engert et al., 2000). Mouse models of ARSACS have been developed that display progressive motor coordination deficits that resemble ataxia (Girard et al., 2012; Lariviere et al., 2015; Lariviere et al., 2019) in ARSACS patients. Misfolding of the protein Sacsin in ARSACS (Kozlov et al., 2011; Menade et al., 2018) is thought to reduce its expression to low or undetectable levels (Lariviere et al., 2019). Sacsin is a multifunctional protein and its absence leads to multiple cellular alterations, including mislocated neurofilaments (Duncan et al., 2017; Gentil et al., 2019; Lariviere et al., 2019), altered chaperone function (Menade et al., 2018), firing deficits in vulnerable Purkinje cells that later die (Ady et al., 2018; Lariviere et al., 2015; Lariviere et al., 2019), and changes in mitochondrial structure and function (Criscuolo et al., 2015; Girard et al., 2012).

Sacsin localizes to both the cytoplasm and mitochondria (Girard et al., 2012). Mitochondrial dysfunction has been observed as a reduction in mitochondrial membrane potential in a mouse model of ARSACS and in patient-derived fibroblasts (Girard et al., 2012). More recently, mitochondrial deficits including reduced mitochondrial respiration and ATP synthesis have been reported in patient-derived fibroblasts (Criscuolo et al., 2015). These results argue that oxidative stress arising from impaired mitochondria, and/or other mitochondrial dysfunction, contribute to ARSACS pathology. This is an intriguing finding, since similar mitochondrial dysfunctions have been reported in several neurodegenerative diseases, including Alzheimer's (AD) and Parkinson's Disease (PD) (Chen and Chan, 2009; Su et al., 2010). Mitochondrial deficits are thought to disrupt cellular function in several manners. For example, the reduction of ATP synthesis observed in ARSACS fibroblasts may be particularly relevant for Purkinje cells in the vulnerable anterior cerebellar vermis in ARSACS. These Purkinje cells fire spontaneous action potentials at high frequencies (Kim et al., 2012;

Abbreviations: ACSF, artificial cerebrospinal fluid; AD, Alzheimer's disease; ARSACS, Autosomal-recessive spastic ataxia of the Charlevoix-Saguenay; CN, cerebellar nuclei; CV, coefficient of variation; MitoQ, mitochondrial-targeted antioxidant ubiquinone or mitoquinone mesylate; PD, Parkinson's Disease; SCA, spinocerebellar ataxia; SOD2, superoxide dismutase 2; WT, wild type.

* Corresponding authors.
E-mail addresses: anne.mckinney@mcgill.ca (R.A. McKinney), alanna.watt@mcgill.ca (A.J. Watt).

https://doi.org/10.1016/j.nbd.2023.106157
Received 26 May 2022; Received in revised form 10 May 2023; Accepted 17 May 2023
Available online 18 May 2023

Zhou et al., 2014), which is energetically costly (Carter and Bean, 2009). Anterior vermis Purkinje cells may thus be more sensitive to ATP depletion, which could explain why these cells are among the most susceptible to cell death in ARSACS (Lariviere et al., 2015; Toscano Marquez et al., 2021). Furthermore, cellular apoptosis is directly regulated by mitochondria, providing a putative mechanism to link mitochondrial deficits with cell death in neurodegenerative diseases (Federico et al., 2012; Tatton and Olanow, 1999).

Given the critical role that mitochondria play in cell health, they have been proposed to be promising therapeutic targets for several neurodegenerative diseases (Angelova et al., 2021; Moreira et al., 2010). One way to target mitochondrial function therapeutically is with mitoquinol mesylate (MitoQ), which enables the antioxidant ubiquinone to accumulate in mitochondria in tissue in vivo, including in the brain (Smith et al., 2003). MitoQ has been shown to be protective against and ameliorate peripheral disease symptoms both preclinically in animal models (Shinn and Lagalwar, 2021; Smith and Murphy, 2010). For example, MitoQ is beneficial in cell and animal models of Huntington disease (Pinho et al., 2020; Yin et al., 2016), AD (McManus et al., 2011; Ng et al., 2014), multiple sclerosis (Mao et al., 2013), amyotrophic lateral sclerosis (Miquel et al., 2014), and PD (Solesio et al., 2013). However, MitoQ was not found to improve symptoms in PD patients (Snow et al., 2010), perhaps because significant neurodegeneration has already occurred in PD patients when symptoms were observed. MitoQ has also been shown to ameliorate neurodegeneration induced by the organophosphate insecticide dichlorvos (Wani et al., 2011). In ataxia, MitoQ has shown some promising results as well. For example, MitoQ prevents cell death in Friedrich's ataxia fibroblasts (Jauslin et al., 2003), as well as in mouse models of the ataxia Spinocerebellar Ataxia type 1 (SCA1), where it improves motor coordination and reduces cell death (Stucki et al., 2016).

Since mitochondrial deficits were among the first cellular alterations identified in a mouse model of ARSACS (Girard et al., 2012), we explored whether MitoQ would be beneficial for slowing or preventing disease progression. To address this, we administered either MitoQ or a sucrose control solution in the drinking water of litter-matched *Sacs*$^{-/-}$ or wildtype (WT) mice for 10 weeks and assessed motor coordination, cerebellar Purkinje cell physiology, mitochondrial structure, and cell counts. We found that chronic MitoQ prevented the worsening of motor coordination deficits, restored levels of superoxide dismutase 2 (SOD2) in cerebellar Purkinje cells and prevented Purkinje cell death. Our findings suggest that MitoQ is a promising therapeutic approach to reduce motor coordination decline in ARSACS.

2. Material and methods

2.1. Animals

We used a mouse model carrying a deletion of the Sacs gene (*Sacs*$^{-/-}$) as previously described (Ady et al., 2018; Lariviere et al., 2015; Toscano Marquez et al., 2021). Heterozygous *Sac*$^{+/-}$ mice were bred to obtain litter-matched *Sacs*$^{-/-}$ and wildtype (WT) control mice. Thus, mice were always compared to litter matched animals. Approximately equal numbers of male and female mice were use in all experiments. Breeding animal procedures were approved by McGill University Animal Care committee in accordance with the regulations by the Canadian Council of Animal Care.

2.2. MitoQ treatment

WT and *Sacs*$^{-/-}$ mice were randomly divided into control and experimental groups after which they were kept single-housed. The animals were provided free access to drinking water containing either 500 mM MitoQ (a gift from Antipodean Pharmaceuticals, San Francisco, CA, USA) diluted in a 5% sucrose (SO389, Sigma, Oakville, ON, Canada) solution or a control 5% sucrose solution, as previously described (Miquel et al., 2014). Solutions were made fresh weekly and cage bottles were refilled every other day, with stock solutions stored at 4 °C between refills. The chronic treatment period lasted for 10 consecutive weeks, similar to drug administration duration in other mouse models of neurodegenerative disease (McManus et al., 2011; Miquel et al., 2014), during which time the animals underwent behavioral testing on the rotarod and elevated beam assays. The daily liquid consumed by mice was recorded each day. While mice consuming MitoQ drank less than mice consuming sucrose solution (**Supplementary Table 1**), there were no significant differences between the amount of MitoQ consumed by WT and *Sacs*$^{-/-}$ mice.

2.3. Behavioral assays

Mice were acclimatized in the behavioral room for 30 min prior to the start of the assays. We used an accelerating protocol on a Rotarod (Stoelting, IITC) as previously described (Jayabal et al., 2016; Jayabal et al., 2015). Briefly, the protocol consisted of a starting speed of 4 rotations per minute (RPM) which accelerated to 40 RPM over 5 min, after which the speed was maintained at 40 RPM for up to an additional 5 min. Prior to commencing MitoQ treatment, animals were trained on the Rotarod apparatus during 3 consecutive days of 4 trials per day, with a 10-min rest period between trials. After which, weekly testing consisted of 4 trials for a single day each week. The latency to fall for each trial was recorded and the average latency to fall for all 4 trials was calculated and reported as the weekly average.

Additionally, an elevated beam assay was administered for the last 4 weeks of the MitoQ treatment (Jayabal et al., 2015). During the first week (week 6 of MitoQ administration), mice were trained to cross a 22 mm round wooden beam. Across following weeks, mice were tested on a 12 mm round wooden beam, with 3 trial per day for two consecutive days each week of treatment. The latency to cross was recorded for each trial and we report the average latency to cross of all the trials per week as the weekly average. We also measured the total number of foot slips that occurred during each week of testing.

2.4. Electrophysiology

Acute cerebellar slices were prepared to allow the measurement of spontaneous Purkinje cell action potentials. Mice were deeply anesthetized inside a chamber with isoflurane. The cerebellum was then dissected and 200 μm sagittal slices of cerebellar vermis were obtain using a VT1200S vibratome (Leica Microsystems, Wetzlar, Germany). Slices were incubated at 37 °C in artificial cerebrospinal fluid (ACSF: 125 mM NaCl, 2.5 mM KCl, 2 mM $CaCl_2$, 1 mM $MgCl_2$, 1.25 mM NaH_2PO_4, 26 mM $NaHCO_3$ and 20 mM glucose, pH set to 7.4 with NaOH; osmolarity ~320 mOsm) bubbled with carbogen mixture (95% O_2 and 5% CO_2) for 40 min and then were maintained at room temperature (~21 °C) until used. Purkinje cells from anterior lobule III in cerebellar vermis were recorded with visual targeting of the electrode to the soma using a cell adjacent extracellular recording configuration. Slices were maintained in ACSF at 33 °C for the duration of the recording. Electrodes were made with borosilicate pipettes pulled with a P-1000 puller (Sutter Instruments, Novato, CA, USA) filled with ACSF. Spike times were analyzed using custom routines in Igor Pro 7.0 (Wavemetrics, Portland, OR, USA).

2.5. Immunohistochemistry

Tissue acquisition was carried out as previously described (Ady et al., 2018; Toscano Marquez et al., 2021). Mice were deeply anesthetized via intracardial perfusion with ice-cold phosphate-buffered saline (PBS, 0.1 M, pH 7.4) with 5.6 μg/mL heparin salt, followed by 40 mL of 4% paraformaldehyde (PFA) in phosphate buffer (PB, 0.1 M, pH 7.4). The cerebellum was dissected and 100 μm vermis and paravermis slices were obtained with a Vibratome 3000 sectioning system (Concord, ON,

Canada). All immunohistochemistry was performed in free floating slices as previously described (Ady et al., 2018; Toscano Marquez et al., 2021). To label Purkinje cell somata and puncta, slices were stained with anti-calbindin antibody (1:500, CB-38a; Swant, Marly, Switzerland) coupled with an Alexa-488 conjugated secondary antibody (1:1000, A32790, Thermo Fisher Scientific, Waltham, MA, USA). To label Purkinje cell puncta with CN neurons, the anti-calbindin antibody described above was used in combination with an anti-NeuN antibody (1:500 abN90, Millipore, Burlington, MA, USA) and a DyLight 405 anti-guinea pig secondary antibody (1:500, 106,475,003, Jackson Immunoresearch, West Grove, PA, USA). Another set of slices was used to label SOD2 using an anti-SOD2 antibody (1:200, ab13534, Abcam, Toronto, ON, Canada) coupled with an Alexa-594 conjugated antibody (1:1000, R37119, ThermoFisher Scientific), in combination with the anti-calbindin antibody described above to identify Purkinje cell bodies. To confirm localization of SOD2 in the mitochondria, we additionally performed double immunohistochemistry with an anti-SOD2 and an Alexa fluor 594 conjugated anti-Tom20 (1:200; ab210665, Abcam) antibody.

2.6. Data acquisition, analysis, and statistics

Images were acquired by a sole researcher blinded to the conditions, using an LSM800 confocal microscope (Zeiss, Toronto, ON, Canada), using Zeiss Zen software for image acquisition. All image analysis was carried out by an experimenter who was blind to the genotype and treatment group of the animal, the gain and contrast were sub-saturating and were kept constant across conditions allowing for comparison of intensities. Image analysis was performed in FIJI (ImageJ; National

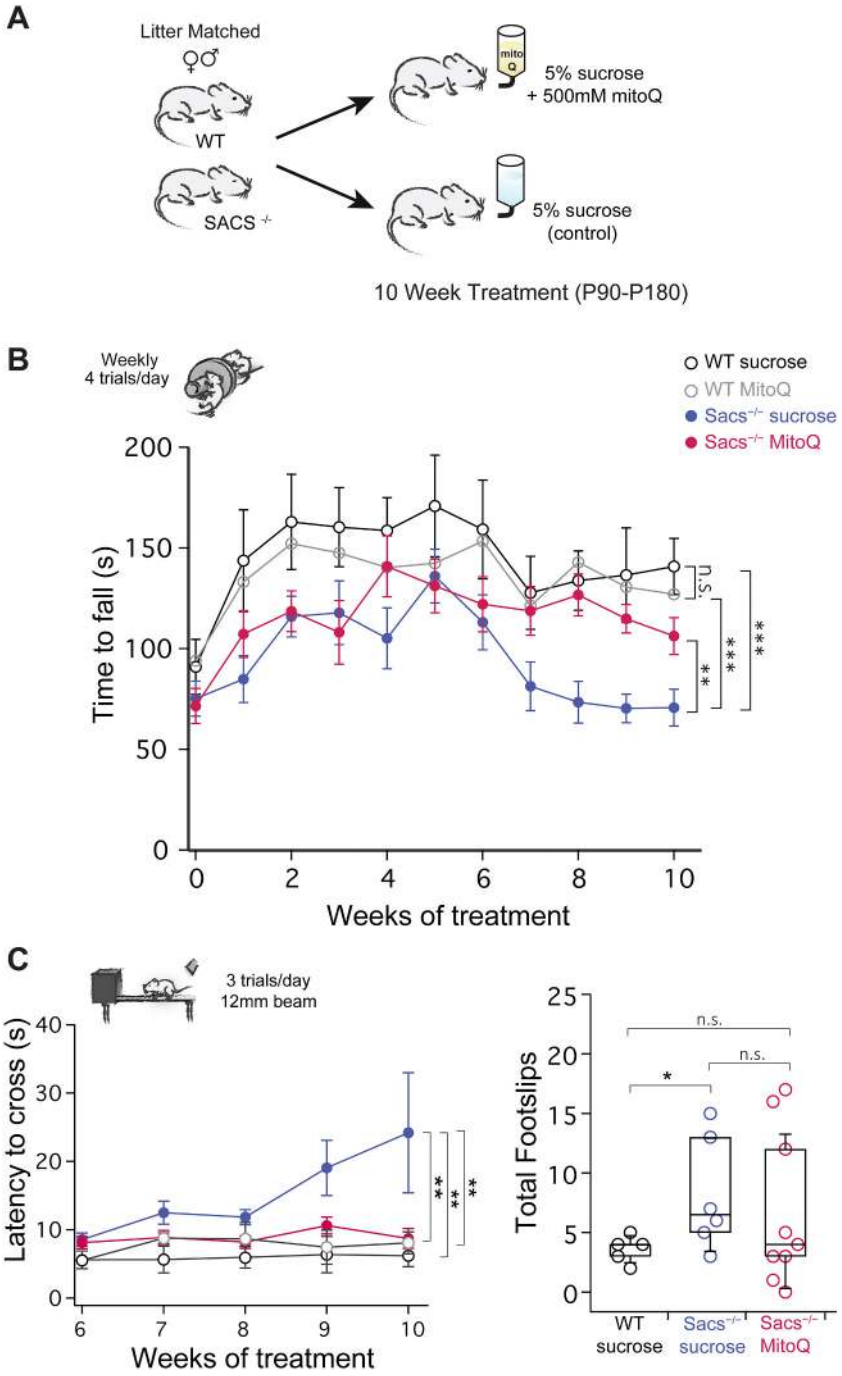

Fig. 1. Chronic MitoQ treatment reduces ataxia in a mouse model of ARSACS. A. Experimental paradigm. B. Weekly rotarod treatment shows that MitoQ-treated *Sacs*$^{-/-}$ mice show significantly better motor coordination after 10 weeks of treatment. WT sucrose: 140 ± 13.8 s; WT MitoQ: 127 ± 9.11 s; *Sacs*$^{-/-}$ sucrose: 70 ± 9.1 s; *Sacs*$^{-/-}$ MitoQ: 106.2 ± 10.9 s. One way ANOVA followed by Tukey's multiple comparisons test performed on last week of treatment followed by Mann Whitney *U* tests. WT sucrose vs WT MitoQ, $P = 0.75$; WT sucrose vs *Sacs*$^{-/-}$ sucrose, $P = 0.001$; WT MitoQ vs *Sacs*$^{-/-}$ sucrose, $P = 0.0006$; WT sucrose vs *Sacs*$^{-/-}$ MitoQ: $P = 0.11$; WT MitoQ vs *Sacs*$^{-/-}$ MitoQ: $P = 0.13$; *Sacs*$^{-/-}$ sucrose vs *Sacs*$^{-/-}$ MitoQ: $P = 0.008$. C. An elevated beam also reveals that *Sacs*$^{-/-}$ mice show improved motor coordination upon MitoQ by reducing the latency to cross (left) and a trend to decrease the number of footslips when crossing (right). Latency to cross of last week of testing: WT sucrose: 8.8 ± 2.3 s; WT MitoQ: 8.8 ± 2.5 s; *Sacs*$^{-/-}$ sucrose: 27.3 ± 2.2 s; *Sacs*$^{-/-}$ MitoQ: 12.4 ± 2.1 s; One-way ANOVA followed by Mann Whitney *U* tests: WT sucrose vs WT MitoQ, $P = 0.51$; WT sucrose vs *Sacs*$^{-/-}$ sucrose, P = 0.001; WT MitoQ, vs *Sacs*$^{-/-}$ sucrose, $P = 0.0002$; WT sucrose vs *Sacs*$^{-/-}$ MitoQ: $P = 0.10$; WT MitoQ vs *Sacs*$^{-/-}$ MitoQ: $P = 0.06$; *Sacs*$^{-/-}$ sucrose vs *Sacs*$^{-/-}$ MitoQ: $P = 0.006$. WT sucrose: $N = 8$; WT MitoQ: $N = 9$; *Sacs*$^{-/-}$ sucrose: $N = 10$; *Sacs*$^{-/-}$ MitoQ: $N = 11$. Footslips: WT sucrose: 3.6 ± 1.5 footslips (fs); *Sacs*$^{-/-}$ sucrose: 8.1 ± 4.9 fs; *Sacs*$^{-/-}$ MitoQ: 11.8 ± 4.0 fs; One-way ANOVA followed by Mann Whitney *U* tests: WT sucrose vs *Sacs*$^{-/-}$ sucrose, $P = 0.026$; WT sucrose vs *Sacs*$^{-/-}$ MitoQ: $P = 0.73$; *Sacs*$^{-/-}$ sucrose vs *Sacs*$^{-/-}$ MitoQ: $P = 0.31$.

Institutes of Health, USA). The Purkinje cell quantification was performed using a single plane image acquired at a 20× magnification and tiled together to get a whole view of lobule III. Purkinje cell density was obtained by quantifying the number of Purkinje cells as a function of the length of the Purkinje cell layer. Images stacks of CN neurons were acquired at a 40× magnification with a 2.0 digital zoom. The cross-section of each cell at the widest point was chosen for analysis. The number of Purkinje cell synapses onto each CN cell was obtained by counting the number of calbindin-positive puncta that were within 0.5 μm of a large CN neuron (>15μm diameter). For SOD2 quantification, images of lobule III of cerebellar vermis taken at a 40 X magnification were used. Manual tracing around Purkinje cell bodies in the calbindin channel allowed the delineation of ROIs around the Purkinje cell bodies. The ROIs were then used in the SOD2 channel and raw fluorescence intensity was measured. The intensity recorded in arbitrary units was normalized to the mean WT value. Statistical analysis was performed using JMP 12 software (SAS, Cary, NC). One-way ANOVAs were used to identify significance, followed by either unpaired Student's *t*-tests for normally distributed data, or Mann Whitney *U* tests when data were not normally distributed. Data are represented by box and whisker plots, showing the median (horizontal line within boxes), second and third quartiles (rectangles) ± 1 SD (whiskers).

3. Results

Since mitochondrial deficits have been suggested as a possible disease-contributing mechanism in *Sacs*$^{-/-}$ mice (Criscuolo et al., 2015; Girard et al., 2012), we wondered whether the mitochondrial-targeted antioxidant ubiquinone MitoQ could improve motor coordination in *Sacs*$^{-/-}$ mice. To test this, we provided either MitoQ in a 5% sucrose solution (MitoQ treatment) or administered 5% sucrose alone as a control (sucrose treatment), in the drinking water of litter-matched *Sacs*$^{-/-}$ and wildtype (WT) mice. Drug administration commenced at postnatal day 90 (P90), an age when motor coordination deficits are observed, and Purkinje cell death is minimally observed (~10% of Purkinje cells in anterior cerebellar cortex have died) (Lariviere et al., 2015)(Fig. 1A). To monitor motor coordination over the duration of the treatment, we measured rotarod performance weekly. We observed that motor coordination increased steeply during the first 2 weeks of treatment in both treated and control WT and *Sacs*$^{-/-}$ mice (Fig. 1B). After 2 weeks, both MitoQ- and sucrose-treated WT mice had largely plateaued, while both MitoQ-treated and control *Sacs*$^{-/-}$ mice continued to show increases in their motor coordination over the next 2–3 weeks, showing that motor learning appears slower in *Sacs*$^{-/-}$ mice, and that MitoQ does not negatively affect motor learning in either WT or *Sacs*$^{-/-}$ mice (Fig. 1B). As treatment persisted beyond 5–6 weeks, however, both WT and *Sacs*$^{-/-}$ mice showed a progressive reduction in motor coordination, with the most severe decline observed in sucrose-treated *Sacs*$^{-/-}$ mice (Fig. 1B). This relatively rapid decline models the progressive nature of ARSACS, and likely reflects accumulating cellular deficits, including increasing levels of Purkinje cell death with time (Lariviere et al., 2015). Remarkably, MitoQ-treated *Sacs*$^{-/-}$ mice showed a significantly lower reduction in motor coordination deficits in the later weeks when compared to sucrose-treated *Sacs*$^{-/-}$ mice (Fig. 1B). These data suggest that MitoQ prevents disease-related decline in motor coordination associated with disease progression in *Sacs*$^{-/-}$ mice but does not affect WT mouse performance on rotarod over the 10 weeks tested.

To further test the effects of MitoQ on motor coordination, we performed an elevated beam assay during the last 4 weeks of drug administration (Fig. 1C). We found that both MitoQ- and sucrose-treated control WT mice were able to cross the elevated beam rapidly (Fig. 1C). *Sacs*$^{-/-}$ mice that were given sucrose had more footslips and a nearly 3-fold increase in the time to cross the beam compared to the WT groups, indicating poorer motor coordination in *Sacs*$^{-/-}$ mice (Fig. 1C). Similar to the improvement demonstrated with rotarod, MitoQ treatment also led to a significant improvement in the time to cross for *Sacs*$^{-/-}$ mice, although performance was not restored to WT levels and the number of footslips was not reduced (Fig. 1C). We observed no significant differences between male and female mice on either rotarod or elevated beam assays (**Supplementary Fig. 1**). Taken together, these data show that 10 weeks of MitoQ treatment significantly reduces motor coordination deficits in a mouse model of ARSACS.

How might MitoQ impact mitochondrial function in *Sacs*$^{-/-}$ mice? It has previously been reported that chronic MitoQ ameliorates mitochondrial function (Jeong et al., 2021; Miquel et al., 2014; Ng et al., 2014), and can upregulate expression of the mitochondrial form of superoxide dismutase 2 (SOD2) (Ning et al., 2021) (Jeong et al., 2021) as well as SOD2 activity (Wani et al., 2011). SOD2 is located on the inner membrane of mitochondria where it removes damaging free radicals like superoxide. Altered SOD2 has been associated with neurodegenerative diseases: its reduction exacerbates AD (Esposito et al., 2006; Li et al., 2004), and it has been implicated in PD (Belluzzi et al., 2012). Furthermore, the presence of disease-associated mutation in ataxin3 are thought to directly reduce the upregulation of SOD2 that can be induced by oxidative stress, suggesting SOD2 dysfunction plays a role in spinocerebellar ataxia type 3 (SCA3)(Araujo et al., 2011). Since motor coordination in ataxia is associated with altered Purkinje cell function in many forms of ataxia (Cook et al., 2021), including ARSACS (Ady et al., 2018; Lariviere et al., 2015; Toscano Marquez et al., 2021), we wondered whether cerebellar Purkinje cell mitochondrial SOD2 might be affected in in *Sacs*$^{-/-}$. To test this, we used immunohistochemistry for anti-calbindin to label cerebellar Purkinje cells (Fig. 2A; shown in aqua, left) as well as anti-SOD2 to label SOD2 (Fig. 2A; shown in purple, right). Although SOD2 is expressed in multiple layers of the cerebellar cortex (Fig. 2A), it is expressed at the highest levels in Purkinje cell somata where it colocalizes with mitochondrial markers (**Supplementary Fig. 2**). We found that SOD2 levels in Purkinje cell somata were reduced in *Sacs*$^{-/-}$ mice compared to WT mice (Fig. 2B), in agreement with previous findings that mitochondrial function is altered in *Sacs*$^{-/-}$ mice. Interestingly, treatment with MitoQ restored SOD2 levels in Purkinje cell somata to WT levels in *Sacs*$^{-/-}$ mice, without affecting WT Purkinje cell expression (Fig. 2B). These results suggest that mitochondrial function in cerebellar Purkinje cells is improved in MitoQ-treated *Sacs*$^{-/-}$ mice and suggests that oxidative stress is likely reduced in cerebellar Purkinje cells.

Altered mitochondrial function and elevated oxidative stress have been linked to cell death in many types of neurodegenerative diseases (Radi et al., 2014), including Friedrich's ataxia, where progressive loss of cerebellar Purkinje cell death is observed (Reichenbach et al., 2002). Progressive Purkinje cell death is a prominent feature observed in both human ARSACS patients and in mouse models of ARSACS, that likely contributes to worsening ataxia (Lariviere et al., 2015; Lariviere et al., 2019; Synofzik et al., 2013; Toscano Marquez et al., 2021). We used immunohistochemistry to label and count Purkinje cells in lobule III of anterior vermis, a cerebellar subregion where cell death is observed at the earliest timepoints (Lariviere et al., 2015) to determine if MitoQ could prevent or reduce cerebellar Purkinje cell death. We observed a significant reduction in Purkinje cell number and a thinner molecular layer in sucrose-treated *Sacs*$^{-/-}$ mice compared to sucrose-treated WT mice (Fig. 3A, B, C), consistent with previous reports (Lariviere et al., 2015). In *Sacs*$^{-/-}$ mice treated with MitoQ, however, Purkinje cell numbers were indistinguishable from WT levels, suggesting that MitoQ was effective in preventing Purkinje cell death in lobule III of *Sacs*$^{-/-}$ mice although molecular layer thickness was not restored (Fig. 3A, B, C; **Supplementary Fig. 3**). MitoQ did not significantly affect WT Purkinje cell counts compared to sucrose-treated control cells, although their numbers were slightly elevated compared to MitoQ-treated *Sacs*$^{-/-}$ mice. These data suggest that MitoQ-treated *Sacs*$^{-/-}$ mice display improved motor coordination perhaps because of the preservation of Purkinje cell numbers in the cerebellum of *Sacs*$^{-/-}$ mice.

We have previously reported that changes in intrinsic firing in anterior cerebellar Purkinje cells precede cell death in *Sacs*$^{-/-}$ mice

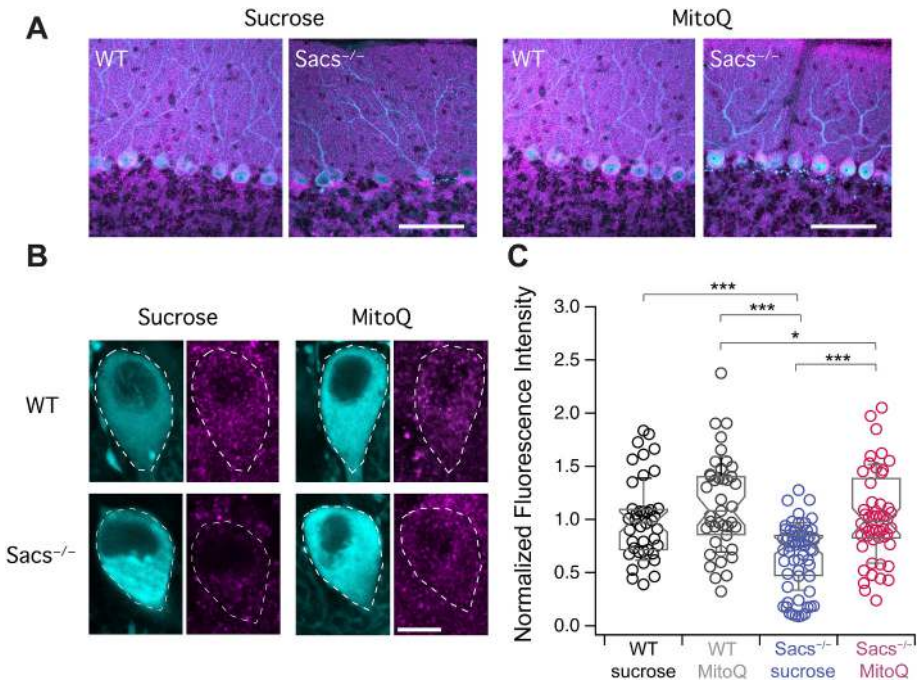

Fig. 2. Chronic MitoQ treatment restores mitochondrial SOD2 in *Sacs*$^{-/-}$ mice. A. Sample images showing expression of SOD2 (purple) and calbindin (cyan) in the cerebellar cortex. Scale bars, 80 μm. B. Sample images showing Purkinje cell somata (left, aqua) and SOD2 expression (right, purple) for WT (top row) and *Sacs*$^{-/-}$ (bottom row) mice either treated with sucrose (left) or MitoQ (right). Scale bars, 10 μm. C. Summary data showing the normalized intensity of somatic SOD2 expression in WT mice is unchanged by MitoQ treatment (black and grey circles) while SOD2 expression is reduced in *Sacs*$^{-/-}$ mice (blue) but is restored to WT levels with chronic MitoQ treatment (pink). Data normalized to WT sucrose expression. One-way ANOVA followed by Mann Whitney *U* tests: WT sucrose vs WT MitoQ, $P = 0.19$; WT sucrose vs *Sacs*$^{-/-}$ sucrose, $P = 0.0004$; WT MitoQ vs *Sacs*$^{-/-}$ sucrose, $P < 0.001$; WT sucrose vs *Sacs*$^{-/-}$ MitoQ: $P = 0.59$; WT MitoQ vs *Sacs*$^{-/-}$ MitoQ: $P = 0.026$; *Sacs*$^{-/-}$ sucrose vs *Sacs*$^{-/-}$ MitoQ: $P = 0.0002$. WT sucrose: $N = 4$ mice, $n = 40$ cells; WT MitoQ: N = 4 mice, $n = 41$ cells; *Sacs*$^{-/-}$ sucrose: $N = 5$ mice, $n = 60$ cells; *Sacs*$^{-/-}$ MitoQ: N = 5 mice, $n = 50$ cells. * $P < 0.05$, ** $P < 0.01$, *** P < 0.001, $P > 0.05$ when not shown. (For interpretation of the references to colour in this figure legend, the reader is referred to the web version of this article.)

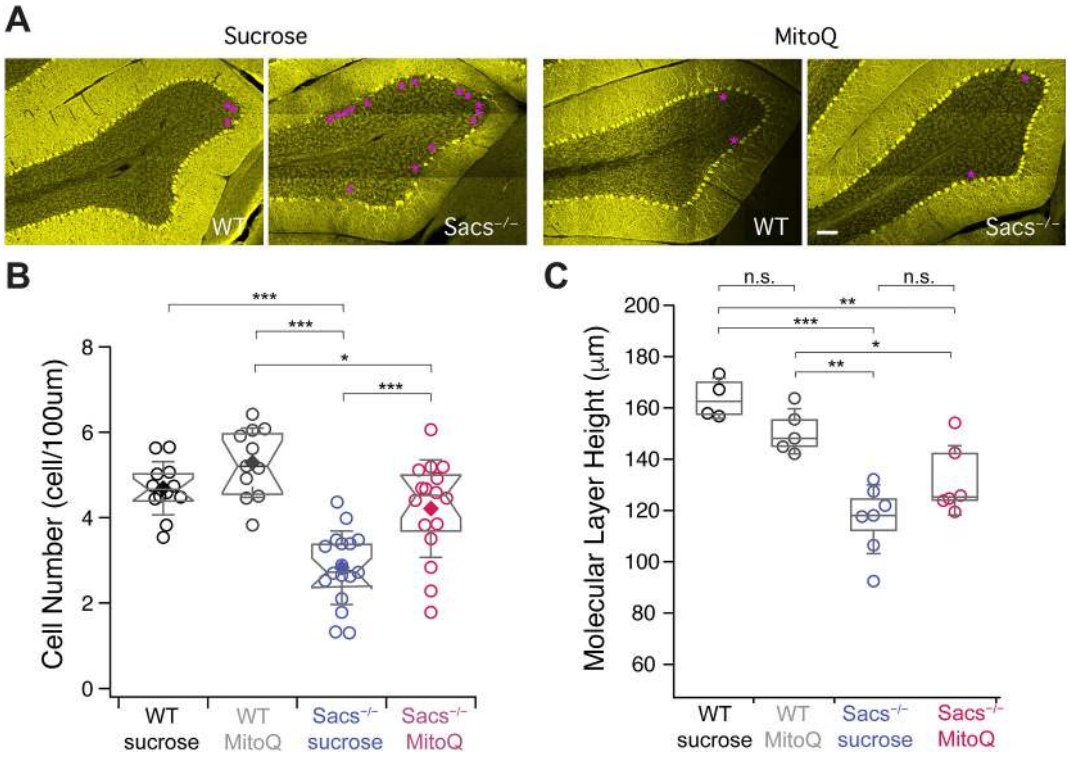

Fig. 3. Chronic MitoQ treatment prevents Purkinje cell death in *Sacs*$^{-/-}$ mice. A. Sample images showing cerebellar Purkinje cells in yellow (labeled with calbindin) in anterior lobule III from WT (top row) and *Sacs*$^{-/-}$ (bottom row) mice either treated with sucrose (left) or MitoQ (right). Gaps in cell layer indicated with magenta asterisks. Scale bar, 100 μm. B. Summary data showing that MitoQ does not affect WT Purkinje cell densities. However, sucrose-treated *Sacs*$^{-/-}$ mice show reduced numbers of Purkinje cells in anterior cerebellar vermis, but this is prevented by chronic MitoQ treatment in *Sacs*$^{-/-}$ mice. C. Summary data showing that molecular layer height is reduced in *Sacs*$^{-/-}$ mice and that MitoQ treatment does not restore this, although the trend is towards an increased height. Cell density: One-way ANOVA followed by Mann Whitney *U* tests: WT sucrose vs WT MitoQ, $P = 0.079$; WT sucrose vs *Sacs*$^{-/-}$ sucrose, $P < 0.001$; WT MitoQ vs *Sacs*$^{-/-}$ sucrose, P < 0.001; WT sucrose vs *Sacs*$^{-/-}$ MitoQ: $P = 0.36$; WT MitoQ vs *Sacs*$^{-/-}$ MitoQ: $P = 0.019$; *Sacs*$^{-/-}$ sucrose vs *Sacs*$^{-/-}$ MitoQ: $P = 0.0007$. WT sucrose: $N = 6$ mice, $n = 12$ images; WT MitoQ: N = 6 mice, $n = 11$ images; *Sacs*$^{-/-}$ sucrose: $N = 8$ mice, $n = 16$ images; *Sacs*$^{-/-}$ MitoQ: N = 8 mice, $n = 17$ images. Molecular layer height: One-way ANOVA followed by Mann Whitney *U* tests: WT sucrose vs WT MitoQ, $P = 0.066$; WT sucrose vs *Sacs*$^{-/-}$ sucrose, P = 0.01; WT MitoQ vs *Sacs*$^{-/-}$ sucrose, $P = 0.005$; WT sucrose vs *Sacs*$^{-/-}$ MitoQ: $P = 0.006$; WT MitoQ vs *Sacs*$^{-/-}$ MitoQ: $P = 0.016$; *Sacs*$^{-/-}$ sucrose vs *Sacs*$^{-/-}$ MitoQ: $P = 0.07$. WT sucrose: N = 6 mice; WT MitoQ: N = 6 mice; *Sacs*$^{-/-}$ sucrose: N = 8 mic; *Sacs*$^{-/-}$ MitoQ: N = 8 mice.*$P < 0.05$; *** P < 0.001, n.s. $P > 0.05$. (For interpretation of the references to colour in this figure legend, the reader is referred to the web version of this article.)

(Ady et al., 2018). Similar changes in Purkinje cell firing properties appear to be a common feature of many ataxias (Cook et al., 2021). Since maintaining elevated firing rates is likely energetically costly to cells (Carter and Bean, 2009), we explored whether improving mitochondrial function with MitoQ would also restore Purkinje cell firing properties. We performed cell-adjacent extracellular recordings from visually identified Purkinje cells in acute cerebellar slices from MitoQ and sucrose-treated *Sacs*$^{-/-}$ and sucrose-treated WT mice (Fig. 4A). We found that Purkinje cells from sucrose-treated WT mice fired action potentials at frequencies that ranged from ~20 to 150 Hz with an average firing frequency of 71 ± 23 Hz (Fig. 4A, B). As we have previously reported (Ady et al., 2018), Purkinje cells from untreated *Sacs*$^{-/-}$ mice fired across a narrower range of frequencies and had significantly lower firing rates (Fig. 4C). Interestingly, treating with MitoQ did not significantly alter the firing rate properties of Purkinje cells from *Sacs*$^{-/-}$ mice (Fig. 4C). In fact, Purkinje cells from MitoQ-treated *Sacs*$^{-/-}$ mice had a narrower range of firing rates and showed significantly reduced firing compared to sucrose-treated WT mouse Purkinje cells (Fig. 4B, C).

Several mouse models of ataxia display firing deficits such as changes in the pacemaker regularity of firing of cerebellar Purkinje cells (Jayabal et al., 2016; Walter et al., 2006). To determine whether such changes are observed in our study, we measured the coefficient of variation (CV) of inter-spike intervals of trains of Purkinje cell action potentials (Fig. 4D). As we have previously reported (Ady et al., 2018), there was no reduction in Purkinje cell regularity observed, since the interspike CV was not significantly altered by MitoQ treatment or genotype (Fig. 4D). These findings suggest that MitoQ does not act therapeutically through the restoration of Purkinje cell firing deficits in *Sacs*$^{-/-}$ mice.

We have previously shown that *Sacs*$^{-/-}$ Purkinje cells have reduced innervation of their target neurons in the cerebellar nuclei (CN) (Ady et al., 2018; Toscano Marquez et al., 2021), which is consistent with previous reports that SOD2-deficient neurons have deficits in distal axonal structure (Misawa et al., 2006). Since CN neurons comprise the projection neurons of the cerebellum, alterations in their input will likely have profound consequences on cerebellar function. We explored whether MitoQ treatment restored Purkinje cell innervation in the CN using immunohistochemistry to label Purkinje cell axonal terminals with calbindin and cell bodies of neurons in the CN with NeuN (Fig. 5A, calbindin in yellow pseudocolour, NeuN in purple pseudocolour). We counted the number of puncta located <0.5 μm of the somata of large CN neurons, and found that their numbers were reduced in sucrose-treated *Sacs*$^{-/-}$ mice compared to sucrose-treated WT mice, consistent with our previous reports (Ady et al., 2018; Toscano Marquez et al., 2021) (Fig. 5B). Interestingly, MitoQ treatment led to a partial restoration in the number of Purkinje cell puncta made onto CN neurons (Fig. 5A, B), although numbers were still lower than in MitoQ- or sucrose-treated WT mice (Fig. 5A, B). Reduced Purkinje cell innervation in the CN concurs with the reduction of Purkinje cell death seen in the MitoQ-treated *Sacs*$^{-/-}$ mice, which is consistent with the hypothesis that the partial restoration of motor coordination in *Sacs*$^{-/-}$ mice arises from decreased Purkinje cell death and the conservation of projections into the neurons in the CN.

4. Discussion

Here we show that 10-week chronic treatment with the mitochondrial-targeted antioxidant ubiquinone, MitoQ, leads to a partial improvement in motor coordination in a mouse model of ARSACS, *Sacs*$^{-/-}$ mice. This takes ~7 weeks to emerge and appears to represent a reduction of disease progression in motor coordination behaviour as observed with rotarod. We observe several cellular changes in the cerebellum after 10 weeks treatment that likely contribute to this

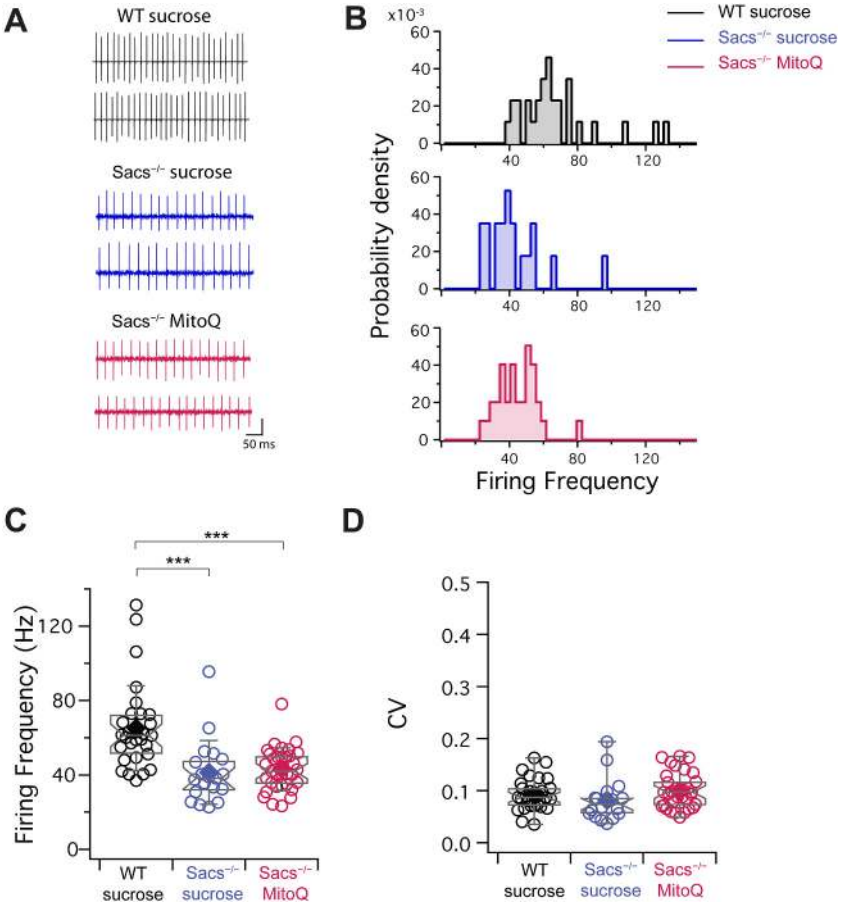

Fig. 4. MitoQ treatment does not restore Purkinje cell firing deficits in *Sacs*$^{-/-}$ mice. A. Sample traces from cell-adjacent recordings taken from Purkinje cells from acute sagittal slices of anterior vermis. B. Histograms showing the distribution of firing rates of Purkinje cells from sucrose-treated WT mice (top, black), sucrose-treated *Sacs*$^{-/-}$ mice (middle, blue) and MitoQ-treated *Sacs*$^{-/-}$ mice (bottom, red). Note that the distribution is shifted to the left in sucrose-treated *Sacs*$^{-/-}$ Purkinje cells, which is similar to the distribution in MitoQ treated *Sacs*$^{-/-}$ mice. C. Firing frequencies are significantly reduced in both sucrose-treated and MitoQ-treated *Sacs*$^{-/-}$ Purkinje cells compared to those from WT mice. WT sucrose: 71 ± 23 Hz; *Sacs*$^{-/-}$ sucrose: 41 ± 17 Hz; *Sacs*$^{-/-}$ MitoQ: 43 ± 12 Hz; ANOVA followed by Tukey's multiple comparison test; WT sucrose vs *Sacs*$^{-/-}$ sucrose: $P = 0.001$; WT sucrose vs *Sacs*$^{-/-}$ MitoQ: $P \leq 0.001$; *Sacs*$^{-/-}$ MitoQ vs *Sacs*$^{-/-}$ sucrose: $P = 0.97$. D. However, firing regularly is not affected in Purkinje cells from *Sacs*$^{-/-}$ mice from either treatment group. WT sucrose: CV = 0.09 ± 0.006; *Sacs*$^{-/-}$ sucrose: CV = 0.08 ± 0.008; *Sacs*$^{-/-}$ MitoQ: CV = 0.10 ± 0.005 Hz; ANOVA followed by Tukey's multiple comparison test; WT sucrose vs *Sacs*$^{-/-}$ sucrose: $P = 0.51$; WT sucrose vs *Sacs*$^{-/-}$ MitoQ: $P = 0.68$; *Sacs*$^{-/-}$ MitoQ vs *Sacs*$^{-/-}$ sucrose: $P = 0.15$. WT sucrose: $N = 4$ mice, $n = 30$ cells; *Sacs*$^{-/-}$sucrose: $N = 3$ mice, $n = 18$ cells; *Sacs*$^{-/-}$ MitoQ: N = 4 mice, 33 cells. *** $P < 0.001$. P > 0.05 when not shown. (For interpretation of the references to colour in this figure legend, the reader is referred to the web version of this article.)

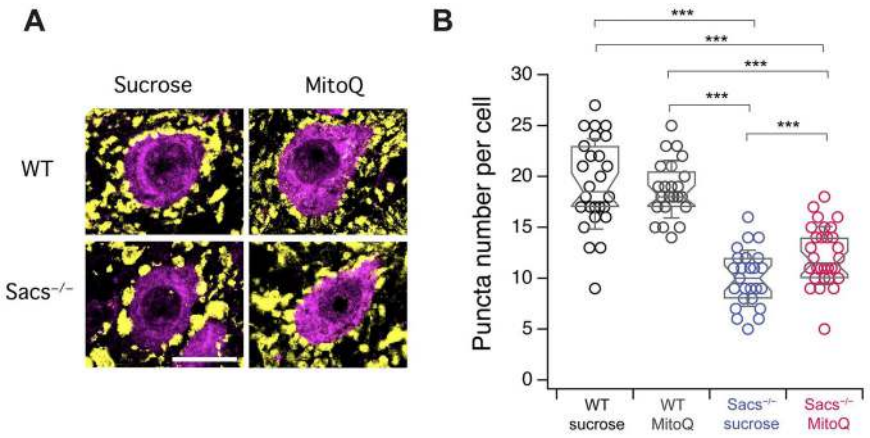

Fig. 5. MitoQ treatment restores Purkinje cell innervation deficits in target neurons in the CN of *Sacs*$^{-/-}$ mice. A. Sample images showing CN neurons (imaged with NeuN in purple pseudo-color) and Purkinje cell puncta located within 0.5 μm proximity of large CN neurons (imaged with calbindin, yellow pseudo-color). Representative images are shown for WT (top) and *Sacs*$^{-/-}$ (bottom) mice, with sucrose-treated (left) and MitoQ-treated (right). Scale bars, 15 μm. B. The number of Purkinje cell puncta in proximity to large CN neuron somata is similar in sucrose-treated (black) and MitoQ-treated (grey) WT mice but is reduced in sucrose-treated *Sacs*$^{-/-}$ mice (blue) and MitoQ-treated *Sacs*$^{-/-}$ mice (bottom, red). Interestingly, MitoQ-treated *Sacs*$^{-/-}$ mice have intermediate Purkinje cell puncta numbers on CN neurons compared to sucrose-treated *Sacs*$^{-/-}$ mice and WT mice. One-way ANOVA followed by Mann Whitney *U* tests: WT sucrose vs WT MitoQ, $P = 0.71$ WT sucrose vs *Sacs*$^{-/-}$ sucrose, $P < 0.001$; WT MitoQ vs *Sacs*$^{-/-}$ sucrose, $P < 0.001$; WT sucrose vs *Sacs*$^{-/-}$ MitoQ: $P < 0.001$; WT MitoQ vs *Sacs*$^{-/-}$ MitoQ: $P < 0.001$; *Sacs*$^{-/-}$ sucrose vs *Sacs*$^{-/-}$ MitoQ: $P = 0.007$. WT sucrose: $N = 3$ mice, $n = 23$ images; WT MitoQ: N = 3 mice, $n = 26$ images; *Sacs*$^{-/-}$sucrose: $N = 4$ mice, $n = 30$ images; *Sacs*$^{-/-}$ MitoQ: N = 4 mice, $n = 25$ images. ** $P < 0.01$, $P > 0.05$ when not shown. (For interpretation of the references to colour in this figure legend, the reader is referred to the web version of this article.)

behavioral rescue. The levels of the mitochondrial antioxidant SOD2 are restored in cerebellar Purkinje cells, suggesting restoration of mitochondrial function. Additionally, the treatment of MitoQ reduced the Purkinje cell death in *Sacs*$^{-/-}$ mice and partially restored innervation by Purkinje cells to their target neurons in the CN. Interestingly, these alterations had no effect on the modification in intrinsic activity that we have observed that precede disease onset in *Sacs*$^{-/-}$ mice (Ady et al., 2018).

MitoQ has been used to improve disease outcomes in multiple cell and animal models of disease. It has been reported to reverse disease presentation and mitochondrial deficits in several neurodegenerative disorders, including in cell and animal models of Huntington disease (Pinho et al., 2020; Yin et al., 2016), AD (McManus et al., 2011; Ng et al., 2014), multiple sclerosis (Mao et al., 2013), amyotrophic lateral sclerosis (Miquel et al., 2014), PD (Solesio et al., 2013), as well as in cell models of ataxia like Friedrich's ataxia (Jauslin et al., 2003), and a mouse model of SCA1 (Stucki et al., 2016). However, these changes have not always translated to human populations, and MitoQ has not been reported to ameliorate disease progression in human PD (Snow et al., 2010). This discrepancy suggests that the timing of MitoQ administration may be important, and that earlier timepoints, which are typically studied in animal models of disease, may not translate well into the clinic.

MitoQ administered systematically is taken up by most tissues of the body, including the brain (Miquel et al., 2014; Smith et al., 2003), thus its actions are likely to be widespread in the organism. While the changes that we observe, such as the reduction in Purkinje cell death, are likely occurring locally, we do not know whether the partial restoration of Purkinje cell innervation in the CN occurs because of improvement of Purkinje cell function, CN neuron function, or both. Since neurons in the CN, like cerebellar Purkinje cells, also express the protein Sacsin that is deleted in ARSACS (Lariviere et al., 2015), it is possible that both brain regions are involved.

A great deal of work from many animal models of ataxia and other cerebellar diseases has linked Purkinje cell firing deficits with Purkinje cell death, since firing deficits typically precede cell death by weeks or months (Cook et al., 2021). This leads to the question of whether firing deficits thus contribute to cell death; that is, whether this correlation in the temporal patterning of disease progression implies causality or not. Here, MitoQ rescued Purkinje cell death without affecting the Purkinje cell firing deficit that we have previously reported precedes cell death (Ady et al., 2018). This suggests then that Purkinje cell firing deficits and Purkinje cell death are not causally linked, but rather tend to occur in a typical order, via distinct mechanisms that can be decoupled from each other. The inability of MitoQ to reverse firing deficits suggests a reason for why its rescue is only partial, given the strong evidence linking firing deficits and ataxia in multiple mouse models (Cook et al., 2021).

Cerebellar Purkinje cells provides a unique set of challenges for protein quantification, since Purkinje cells are large but relatively rare, making up <2% of the total cerebellar cell number, which is dominated by the small, numerous cerebellar granule cells. While techniques like ELISA are considered the gold standard of protein quantification, ELISA requires tissue homogenates where changes in Purkinje cell proteins will be diluted. In contrast quantitative immunohistochemistry allows the measurement of relative protein levels in specific cell types, and has been shown in fact to be more sensitive than ELISA for detecting changes in proteins in subsets of specific cells (Jensen et al., 2017), including cerebellar Purkinje cells (Cook et al., 2021). Hence in this study we employed immunohistochemistry to semi-quantitatively measure changes in the Purkinje cell mitochondrial protein SOD2.

Cellular antioxidants are tightly regulated in cells, including in mitochondria. Both down-regulation and up-regulation of SOD2 have been observed in disease, which are both thought to contribute to mitochondrial dysfunction (Flynn and Melov, 2013). Remarkably, MitoQ has been shown to upregulate SOD2 expression both when it is abnormally upregulated already in a cellular model of vascular fibrosis (Ning et al., 2021), and in a mouse model of aging where SOD2 levels are reduced (Jeong et al., 2021). Our findings suggest that the normalization of SOD2 with chronic MitoQ treatment may reduce mitochondrial oxidative stress in *Sacs*$^{-/-}$ mice, at least in Purkinje cell somata.

Previous reports have found that Purkinje cell death in *Sacs*$^{-/-}$ mice occurs predominantly in anterior lobules of the cerebellar vermis (Lariviere et al., 2019), where cell death is restricted to Purkinje cells that do not express zebrin, which accounts for >85% of Purkinje cells in lobule III (Toscano Marquez et al., 2021). Consistent with this, we observed a significant reduction of Purkinje cell death in lobule III of the vermis in MitoQ-treated *Sacs*$^{-/-}$ mice. However, we cannot rule out the possibility that MitoQ does not rescue Purkinje cell death uniformly in all lobules of the anterior vermis. A stereological approach would be required to address this question (Golub et al., 2015; Schmitz and Hof, 2005). Without stereology, caution should be taken to not generalize results from lobule III to other anterior vermal lobules.

At present, there are unfortunately no viable treatment options for ARSACS meaning that research such as our study that identifies novel

therapeutic strategies for ARSACS is important. However, caution needs to be employed in the interpretation of our results and how they may translate to the clinic. For instance, we have shown that MitoQ prevents Purkinje cell death in part of anterior vermis that is thought to contribute to disease progression. Our results suggest that MitoQ may be most effective therapeutically if administered at early disease timepoints before significant cell death has occurred. It is unclear whether MitoQ can ameliorate disease progression after Purkinje cell death has taken place. In humans, disease progression occurs over months and years rather than weeks, which should be considered when designing future clinical trials. Nonetheless, MitoQ shows great promise for ARSACS, and its therapeutic actions can be linked to brain pathophysiology that a great deal of work suggests contributes to disease pathophysiology in ataxia.

5. Conclusions

In this article, we investigate the effects of the mitochondrial-targeted antioxidant MitoQ on ataxia and cerebellar deficits in a mouse model of ARSACS. We use male and female *Sacs*$^{-/-}$ and WT control mice that are treated with either sucrose or MitoQ and find that MitoQ prevents the progression of ataxia and improves motor coordination in *Sacs*$^{-/-}$ mice without affecting WT mice. This improvement is accompanied by restoring the expression of the mitochondrial antioxidant SOD2, by reducing cerebellar Purkinje cell death in anterior cerebellum, and by partially reversing the innervation deficits in the CN. These results argue that MitoQ might be a viable therapy for ARSACS patients.

Funding sources

This work was funded by a Project grant from the ARSACS Foundation (AJW and RAM), and the Canadian Institutes of Health Research Project Grant (AJW).

Credit author

B.T.M. helped conceive of the project, performed most of the experiments, analyzed data, made figures, and co-wrote the manuscript. J. H. performed experiments for Figs. 1 and 3. S. L. helped with experiments and analysis. F. C. helped with experiments and analysis. R.A.M. and A.J.W. helped conceive of and supervise the project and co-wrote the manuscript.

Declaration of Competing Interest

The authors state that there are no conflicts of interest in connection with this article.

Data availability

Data will be made available on request.

Acknowledgements

We thank the past and present members of the Watt and McKinney labs for constructive feedback on this data and manuscript and support and advice throughout this project. We thank Tanya Koch and the McGill Comparative Medicine and Animal Resources Centre for technical help with animal colony maintenance. We thank Jesper Sjöström for help with custom Igor code for electrophysiology data acquisition and analysis. We thank Siegfried Hekimi and members of the Hekimi lab for helpful discussions and technical resources for this project. We thank the Advanced BioImaging Facility at McGill University for technical support with image acquisition and analysis. We thank Antipodean Pharmaceuticals for the generous gift of MitoQ. We are grateful for the support from Sonia Gobeil and the ARSACS Foundation for this work.

Appendix A. Supplementary data

Supplementary data to this article can be found online at https://doi.org/10.1016/j.nbd.2023.106157.

References

Ady, V., et al., 2018. Altered synaptic and intrinsic properties of cerebellar Purkinje cells in a mouse model of ARSACS. J. Physiol. 596, 4253–4267.
Angelova, P.R., et al., 2021. Mitochondria and lipid peroxidation in the mechanism of neurodegeneration: finding ways for prevention. Med. Res. Rev. 41, 770–784.
Araujo, J., et al., 2011. FOXO4-dependent upregulation of superoxide dismutase-2 in response to oxidative stress is impaired in spinocerebellar ataxia type 3. Hum. Mol. Genet. 20, 2928–2941.
Belluzzi, E., et al., 2012. Human SOD2 modification by dopamine quinones affects enzymatic activity by promoting its aggregation: possible implications for Parkinson's disease. PLoS One 7, e38026.
Bouchard, J.P., et al., 1978. Autosomal recessive spastic ataxia of Charlevoix-Saguenay. Can. J. Neurol. Sci. 5, 61–69.
Carter, B.C., Bean, B.P., 2009. Sodium entry during action potentials of mammalian neurons: incomplete inactivation and reduced metabolic efficiency in fast-spiking neurons. Neuron. 64, 898–909.
Chen, H., Chan, D.C., 2009. Mitochondrial dynamics–fusion, fission, movement, and mitophagy–in neurodegenerative diseases. Hum. Mol. Genet. 18, R169–R176.
Cook, A.A., et al., 2021. Losing the beat: contribution of Purkinje cell firing dysfunction to disease, and its reversal. Neuroscience. 462, 247–261.
Criscuolo, C., et al., 2015. Powerhouse failure and oxidative damage in autosomal recessive spastic ataxia of Charlevoix-Saguenay. J. Neurol. 262, 2755–2763.
Duncan, E.J., et al., 2017. Altered organization of the intermediate filament cytoskeleton and relocalization of proteostasis modulators in cells lacking the ataxia protein sacsin. Hum. Mol. Genet. 26, 3130–3143.
Engert, J.C., et al., 2000. ARSACS, a spastic ataxia common in northeastern Quebec, is caused by mutations in a new gene encoding an 11.5-kb ORF. Nat. Genet. 24, 120–125.
Esposito, L., et al., 2006. Reduction in mitochondrial superoxide dismutase modulates Alzheimer's disease-like pathology and accelerates the onset of behavioral changes in human amyloid precursor protein transgenic mice. J. Neurosci. 26, 5167–5179.
Federico, A., et al., 2012. Mitochondria, oxidative stress and neurodegeneration. J. Neurol. Sci. 322, 254–262.
Flynn, J.M., Melov, S., 2013. SOD2 in mitochondrial dysfunction and neurodegeneration. Free Radic. Biol. Med. 62, 4–12.
Gentil, B.J., et al., 2019. Sacsin, mutated in the ataxia ARSACS, regulates intermediate filament assembly and dynamics. FASEB J. 33, 2982–2994.
Girard, M., et al., 2012. Mitochondrial dysfunction and Purkinje cell loss in autosomal recessive spastic ataxia of Charlevoix-Saguenay (ARSACS). Proc. Natl. Acad. Sci. U. S. A. 109, 1661–1666.
Golub, V.M., et al., 2015. Neurostereology protocol for unbiased quantification of neuronal injury and neurodegeneration. Front. Aging Neurosci. 7, 196.
Jauslin, M.L., et al., 2003. Mitochondria-targeted antioxidants protect Friedreich Ataxia fibroblasts from endogenous oxidative stress more effectively than untargeted antioxidants. FASEB J. 17, 1972–1974.
Jayabal, S., et al., 2015. Rapid onset of motor deficits in a mouse model of spinocerebellar ataxia type 6 precedes late cerebellar degeneration. eNeuro. 2, 1–18.
Jayabal, S., et al., 2016. 4-aminopyridine reverses ataxia and cerebellar firing deficiency in a mouse model of spinocerebellar ataxia type 6. Sci. Rep. 6, 29489.
Jensen, K., et al., 2017. A novel quantitative immunohistochemistry method for precise protein measurements directly in formalin-fixed, paraffin-embedded specimens: analytical performance measuring HER2. Mod. Pathol. 30, 180–193.
Jeong, J.H., et al., 2021. Neuroprotective benefits of exercise and MitoQ on memory function, mitochondrial dynamics, oxidative stress, and neuroinflammation in D-Galactose-Induced aging rats. Brain Sci. 11.
Kim, C.H., et al., 2012. Lobule-specific membrane excitability of cerebellar Purkinje cells. J. Physiol. 590, 273–288.
Kozlov, G., et al., 2011. Structural basis of defects in the sacsin HEPN domain responsible for autosomal recessive spastic ataxia of Charlevoix-Saguenay (ARSACS). J. Biol. Chem. 286, 20407–20412.
Lariviere, R., et al., 2015. Sacs knockout mice present pathophysiological defects underlying autosomal recessive spastic ataxia of Charlevoix-Saguenay. Hum. Mol. Genet. 24, 727–739.
Lariviere, R., et al., 2019. Sacs R272C missense homozygous mice develop an ataxia phenotype. Mol. Brain. 12, 19.
Li, F., et al., 2004. Increased plaque burden in brains of APP mutant MnSOD heterozygous knockout mice. J. Neurochem. 89, 1308–1312.
Mao, P., et al., 2013. MitoQ, a mitochondria-targeted antioxidant, delays disease progression and alleviates pathogenesis in an experimental autoimmune encephalomyelitis mouse model of multiple sclerosis. Biochim. Biophys. Acta 1832, 2322–2331.
McManus, M.J., et al., 2011. The mitochondria-targeted antioxidant MitoQ prevents loss of spatial memory retention and early neuropathology in a transgenic mouse model of Alzheimer's disease. J. Neurosci. 31, 15703–15715.

Menade, M., et al., 2018. Structures of ubiquitin-like (Ubl) and Hsp90-like domains of sacsin provide insight into pathological mutations. J. Biol. Chem. 293, 12832–12842.
Miquel, E., et al., 2014. Neuroprotective effects of the mitochondria-targeted antioxidant MitoQ in a model of inherited amyotrophic lateral sclerosis. Free Radic. Biol. Med. 70, 204–213.
Misawa, H., et al., 2006. Conditional knockout of Mn superoxide dismutase in postnatal motor neurons reveals resistance to mitochondrial generated superoxide radicals. Neurobiol. Dis. 23, 169–177.
Moreira, P.I., et al., 2010. Mitochondria: a therapeutic target in neurodegeneration. Biochim. Biophys. Acta 1802, 212–220.
Ng, L.F., et al., 2014. The mitochondria-targeted antioxidant MitoQ extends lifespan and improves healthspan of a transgenic *Caenorhabditis elegans* model of Alzheimer disease. Free Radic. Biol. Med. 71, 390–401.
Ning, R., et al., 2021. The mitochondria-targeted antioxidant MitoQ attenuated PM2.5-induced vascular fibrosis via regulating mitophagy. Redox Biol. 46, 102113.
Pinho, B.R., et al., 2020. The interplay between redox signalling and proteostasis in neurodegeneration: in vivo effects of a mitochondria-targeted antioxidant in Huntington's disease mice. Free Radic. Biol. Med. 146, 372–382.
Radi, E., et al., 2014. Apoptosis and oxidative stress in neurodegenerative diseases. J. Alzheimers Dis. 42 (Suppl. 3), S125–S152.
Reichenbach, J., et al., 2002. Elevated oxidative stress in patients with ataxia telangiectasia. Antioxid. Redox Signal. 4, 465–469.
Schmitz, C., Hof, P.R., 2005. Design-based stereology in neuroscience. Neuroscience. 130, 813–831.
Shinn, L.J., Lagalwar, S., 2021. Treating neurodegenerative disease with antioxidants: efficacy of the bioactive phenol resveratrol and mitochondrial-targeted MitoQ and SkQ. Antioxidants (Basel). 10.
Smith, R.A., Murphy, M.P., 2010. Animal and human studies with the mitochondria-targeted antioxidant MitoQ. Ann. N. Y. Acad. Sci. 1201, 96–103.
Smith, R.A., et al., 2003. Delivery of bioactive molecules to mitochondria in vivo. Proc. Natl. Acad. Sci. U. S. A. 100, 5407–5412.
Snow, B.J., et al., 2010. A double-blind, placebo-controlled study to assess the mitochondria-targeted antioxidant MitoQ as a disease-modifying therapy in Parkinson's disease. Mov. Disord. 25, 1670–1674.
Solesio, M.E., et al., 2013. The mitochondria-targeted anti-oxidant MitoQ reduces aspects of mitochondrial fission in the 6-OHDA cell model of Parkinson's disease. Biochim. Biophys. Acta 1832, 174–182.
Stucki, D.M., et al., 2016. Mitochondrial impairments contribute to spinocerebellar ataxia type 1 progression and can be ameliorated by the mitochondria-targeted antioxidant MitoQ. Free Radic. Biol. Med. 97, 427–440.
Su, B., et al., 2010. Abnormal mitochondrial dynamics and neurodegenerative diseases. Biochim. Biophys. Acta 1802, 135–142.
Synofzik, M., et al., 2013. Autosomal recessive spastic ataxia of Charlevoix Saguenay (ARSACS): expanding the genetic, clinical and imaging spectrum. Orphan. J. Rare Dis. 8, 41.
Tatton, W.G., Olanow, C.W., 1999. Apoptosis in neurodegenerative diseases: the role of mitochondria. Biochim. Biophys. Acta 1410, 195–213.
Toscano Marquez, B., et al., 2021. Molecular identity and location influence Purkinje cell vulnerability in autosomal-recessive spastic Ataxia of Charlevoix-Saguenay mice. Front. Cell. Neurosci. 15, 707857.
Walter, J.T., et al., 2006. Decreases in the precision of Purkinje cell pacemaking cause cerebellar dysfunction and ataxia. Nat. Neurosci. 9, 389–397.
Wani, W.Y., et al., 2011. Protective efficacy of mitochondrial targeted antioxidant MitoQ against dichlorvos induced oxidative stress and cell death in rat brain. Neuropharmacology. 61, 1193–1201.
Yin, X., et al., 2016. Mitochondria-targeted molecules MitoQ and SS31 reduce mutant huntingtin-induced mitochondrial toxicity and synaptic damage in Huntington's disease. Hum. Mol. Genet. 25, 1739–1753.
Zhou, H., et al., 2014. Cerebellar modules operate at different frequencies. Elife. 3, e02536.